DOI: 10.1002/ejic.200800626

Isomeric Al_2R_4, Mg_2R_2 Species and Oligomerisation Products: Investigation of Al–Al and Mg–Mg σ Bonding

Tobias Pankewitz,[a] Wim Klopper,*[a] Patrick Henke,[b] and Hansgeorg Schnöckel*[b]

Keywords: Aluminum / Magnesium / Metal–metal σ bonding / Diradicals / Ab initio calculations / Stability analysis / Low-valent metal compounds

Initiated by ongoing experimental work in the field of subvalent aluminium compounds and by recent results on isoelectronic Mg_2R_2 (s^1 states) species, detailed theoretical work was necessary to explain the unusual bonding situation in some Al_2R_4 isomers (R = P*t*Bu$_2$), of a dimeric $Al_4R'_8$ (R′ = O*t*Bu) as well as of subhalides Al_2F_4, Al_2Cl_4, Mg_2Cl_2 and some of their oligomers. These results are presented in this contribution. Especially the different isomers of the four-membered heterocyclic $RAlR_2AlR$ molecule needed careful theoretical investigation, since on the way from monomeric AlR_2 radicals to the most stable $RAlR_2AlR$ isomer with a butterfly shape, intermediates with different Al–Al interactions – exhibiting diradical as well as diradicaloid character – have to be considered. The presented results on the unusual bonding in these AlP_2Al four-membered heterocyclic systems are an important contribution to a better understanding of the bonding situations in many inorganic molecules containing, for example, B_2P_2, C_2P_2, Ge_2N_2, Sn_2N_2 and Si_4 entities, which recently have drawn considerable interest. In analogy to the Al^{II} compounds some isoelectronic Mg^{I} species have been investigated. Regarding the obtained results, special attention is drawn to MgCl oligomers, since we found unexpectedly high oligomerisation energies in our calculations. This high stabilisation is based on direct Mg–Mg bonding as well as on Mg–Cl–Mg bridging bonds. These mixed bonding motifs may also be present in the so far unknown solid MgCl.

I. Introduction

Compounds containing metal–metal bonds of main group elements have gained increased interest in recent times. Most remarkable are the results for the first molecules that contain a 2-electron-2-centre Mg–Mg or Zn–Zn bond,[1,2] which have been published as highlight articles.[3,4] Although theoretically Al^{II} is isoelectronic with Mg^{I} present in crystalline $Mg_2R'_2$ species,[2] the corresponding Al_2R_4 [R = $CH(SiMe_3)_2$][5] and $Al_2X_4{\cdot}2L$ (X = Cl, Br; L = ether or amine)[6,7] molecules that were presented about 20 years ago seem to be less interesting. However, as far as we know, neither Mg^{I} nor Al^{II} or Ga^{II} monomeric radical species like $^{\cdot}MgR$, $^{\cdot}MgX$ or $^{\cdot}AlR_2$, $^{\cdot}AlX_2$ have been identified as crystalline materials.

In order to understand the formation of Mg–Mg as well as of Al–Al bonds during the synthesis of Mg_2R_2 and Al_2R_4 species, it seems necessary to invoke intermediates in which the ligands are allowed to show different bonding motifs between terminal and bridging positions. On the basis of first results from ongoing experiments with two unusually bonded Al_2R_4 molecules,[8] we present here detailed theoretical investigations of various Al_2R_4 isomers and their disproportionation. Motivated by our experimental results, we shall first investigate the aluminium systems. We shall then address the isoelectronic magnesium systems, which have recently been subject to several theoretical studies and discussions, especially concerning the structure and bonding of Mg_2Cp_2 and further metal-rich Cp species.[9,10] We shall show here that even the binary species MgCl is worth to be investigated. In order to elucidate the structure and bonding of this so far nonexisting solid compound, we have investigated the structure of the MgCl oligomers, their thermodynamic behaviour with respect to disproportionation to solid magnesium metal and $MgCl_2$ and in relation to the formation of the hypothetical solid MgCl.

II. Results and Discussion

II.A. $Al_2(PtBu_2)_4$ Isomers

II.A.1. The Butterfly Motif

In contrast to the first examples of Al–organic compounds with Al–Al bonds, we have found a butterfly structure in ongoing experiments in our laboratory with phosphorus-based ligands. The ground-state structural parameters of this butterfly isomer of $Al_2(PtBu_2)_4$ (**1**) (C_2 sym-

[a] Center for Functional Nanostructures (CFN) and Lehrstuhl für Theoretische Chemie, Institut für Physikalische Chemie, Universität Karlsruhe (TH),
76128 Karlsruhe, Germany
E-mail: klopper@chem-bio.uni-karlsruhe.de
[b] Center for Functional Nanostructures (CFN) and Institut für Anorganische Chemie, Universität Karlsruhe (TH),
76128 Karlsruhe, Germany
E-mail: hansgeorg.schnoeckel@chemie.uni-karlsruhe.de

metry, ^{1}A state) calculated at the level of density functional theory (DFT) with the functionals BP86, TPSS and B3LYP are compared to the X-ray structure in Table 1.[8] The overall structure is shown in Figure 1 (see Figure 2 for the numbering of atoms).

Table 1. Calculated structural parameters for $Al_2(PtBu_2)_4$ isomer **1** and TS **1**‡. Selected bond lengths [pm], bond angles [°] and corresponding experimental values in the crystal; for atom numbers, see Figure 2. Geometries are optimised by using the functionals BP86, TPSS and B3LYP with a def2-TZVP basis for Al, P and a def2-SV(P) basis for C, H. An imaginary frequency of 11*i* cm^{-1} was calculated with BP86 for TS **1**‡, corresponding to the "butterfly movement" of the molecule.

	1				**1**‡		
	Exptl.	BP86	TPSS	B3LYP	BP86	TPSS	B3LYP
Al1–Al2	258.7	261.8	259.6	258.6	305.1	303.6	302.6
Al1–P1	237.0	240.6	239.7	240.2	238.6	238.1	238.4
Al1–P2	236.2	239.8	239.5	240.2	234.8	234.3	233.7
Al2–P2	242.2	245.2	245.0	246.1	235.2	234.7	234.2
Al1–P2–Al2	65.4	65.3	64.7	64.2	80.9	80.7	80.6
P2–Al1–P3	94.5	95.1	94.8	95.5	99.1	99.3	99.4
P1–Al1–Al2	160.9	160.2	159.6	160.7	166.7	166.7	167.7

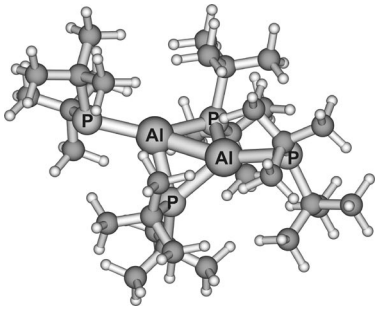

Figure 1. Structure of butterfly $Al_2(PtBu_2)_4$ isomer **1** (C_2 symmetry, ^{1}A state). Al and P atoms are indicated.

The bonding motif is an $Al(P_b)_2Al$ butterfly (P_b: bridging phosphorus) with a direct Al–Al σ bond (bow-shaped highest occupied molecular orbital, HOMO) of 258.6 pm to 261.8 pm depending on the functional. There are two $PtBu_2$ groups bridging the two aluminium atoms and two terminally attached $PtBu_2$ groups. The geometry optimisation of **1** turned out to be very demanding, and it thus became clear that the potential energy surface of the molecule is complicated, with a number of close-lying local minima. Besides calculated conformer **1**, which fits the experimental X-ray structure and which we feel is the global minimum, we have identified several other butterfly conformers within a range of 27 kJ mol^{-1}. Two of these conformers are depicted in Figure 3. In all structures, the terminal $P(tBu)_2$ groups are bent with respect to the Al–Al axis. In conformer **1a** (C_2 symmetry), which lies 5–7 kJ mol^{-1} above the global minimum (depending on the functional), the longer of the two Al–P_b bonds with the same aluminium atom (i.e., the Al1–P2 bond) coincides with the hemisphere of the

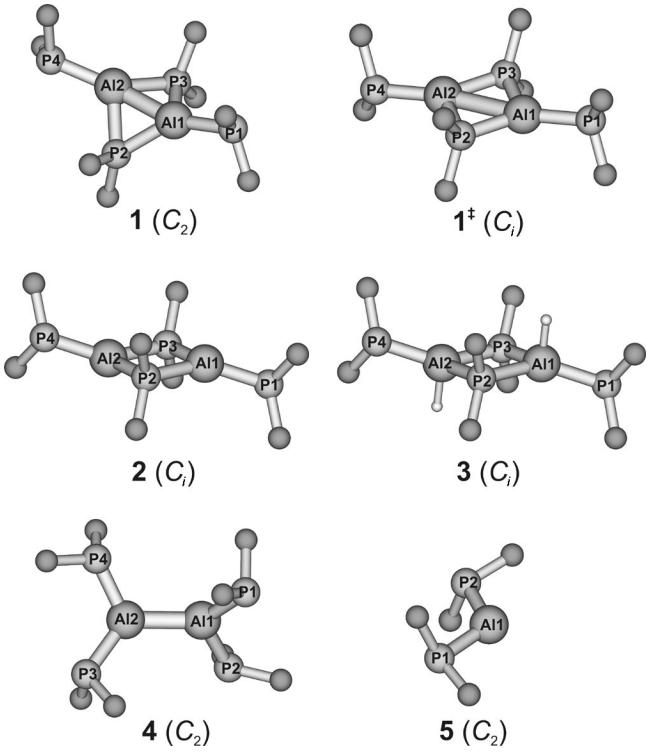

Figure 2. Structures of the $Al_2(PtBu_2)_4$ isomers: butterfly structure **1** (C_2 symmetry, ^{1}A), TS **1**‡ (C_i symmetry) between the two equivalent butterfly structures, triplet structure **2** (C_i symmetry, ^3A_u), H-saturated isomer **3** (C_i symmetry, ^1A_g), linear isomer **4** (C_2 symmetry, ^{1}A) and radical fragment **5** (C_2 symmetry, ^{2}A). For clarity, only the tertiary carbon atoms of the *t*Bu groups are shown.

butterfly where the sterically demanding *t*Bu groups of the terminal $P(tBu)_2$ group are located. The shorter Al–P_b bonds are on the side of the molecule where the lone pairs of the terminal $P(tBu)_2$ groups reside. In the X-ray and calculated global minimum structure **1**, the bonding situation is exactly the opposite (see Figure 3). Here, the longer Al–P_b bond is found on the side of the lone electron pair.

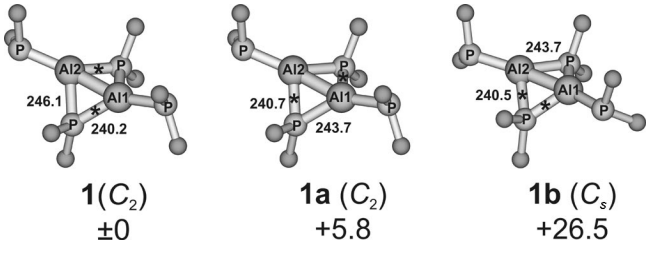

Figure 3. The global minimum structure, **1**, and two energetically low-lying conformers, **1a** and **1b**, of the $Al_2(PtBu_2)_4$ butterfly isomer. Bond lengths [pm] at the B3LYP/def2-TZVP† level of theory. The shorter bonds within the four-membered ring are indicated by a star. Energy differences are in kJ mol^{-1}. For clarity, only the tertiary carbon atoms of the *t*Bu groups are shown.

We have also calculated conformer **1b**, in which both terminal $P(tBu)_2$ groups are bent to the same side and the lone pairs of the P_t (terminal phosphorus) point in the same direction (C_s symmetry). In this case, the two short Al–P_b

bonds are on the same side of the butterfly, and the long Al–P_b bonds coincide with the hemisphere in which all *t*Bu groups are located. Energetically, this conformer lies 24–27 kJ mol^{-1} above the global minimum structure, **1**.

We conclude from these observations that the molecule with its overall spherical shape is more or less space-filled and that any rotation of groups reducing steric hindrance on one side will increase it on the other. This leads to a situation of various energetically close-lying conformers.

In addition, the optimised geometry of structure **1**‡, which is the transition state (TS) between two equivalent forms of butterfly **1**, is reported in Table 1 and displayed in Figure 2. The one and only imaginary frequency of 11*i* cm^{-1} at the BP86/def2-TZVP† level of theory corresponds to a flipping between the two equivalent butterfly structures, which are separated by a barrier of 24.0 kJ mol^{-1} (B3LYP/def2-TZVP). This flipping can be described as the up-and-down movement of the butterfly's wings. Along this movement, the Al–Al σ bond of the butterfly opens and becomes a π orbital in the TS. Then, a new Al–Al σ bond is formed on the opposite side of the $Al(P_b)_2Al$ plane, leading to the inverted butterfly.

II.A.2. The Four-Membered-Ring Motif

We have synthesised a second isomer of $Al_2(PtBu_2)_4$, which is a four-membered-ring structure with an Al–Al distance of 350.8 pm in the crystal (Table 2). This much longer Al–Al distance relative to the value of 258.7 pm in butterfly **1** suggests the absence of a direct Al–Al bond. In Table 2, we compare the experimental structural data with a calculated geometry of a diradical four-membered-ring structure, **2** [C_i symmetry, ^3A_u state, with a p-shaped singly occupied molecular orbital (SOMO) at each aluminium atom], and with the calculated geometry of hypothetical compound **3**, where the two SOMOs are saturated with two hydrogen atoms (C_i symmetry, ^1A_g state). The overall structures and numbering of atoms are given in Figure 2.

Table 2. Calculated structural parameters for triplet $Al_2(PtBu_2)_4$ (**2**) and H-saturated singlet compound **3** are compared to experimental values for the four-membered-ring structure. Selected bond lengths [pm] and bond angles [°] are given; for atom numbers, see Figure 2. Geometries are optimised by using the functionals BP86, TPSS and B3LYP with a def2-TZVP basis for Al, P and a def2-SV(P) basis for C, H.

	Exptl.	**2**			**3**		
		BP86	TPSS	B3LYP	BP86	TPSS	B3LYP
Al1–Al2	350.8	346.2	344.9	348.7	357.7	357.6	358.6
Al1–P1	239.9	239.1	238.3	239.5	243.1	242.3	242.8
Al1–P2	247.8	245.0	244.6	246.2	251.9	251.5	252.6
Al2–P2	245.8	243.9	243.6	245.0	250.1	249.8	250.7
Al1–P2–Al2	90.5	90.2	89.9	90.4	90.9	91.0	90.9
P2–Al1–P3	89.4	89.9	90.1	89.5	89.1	89.0	89.1
P1–Al1–Al2	151.7	154.1	154.4	152.5	152.9	152.8	152.1

Saturating diradical **2** with hydrogen atoms to form closed-shell molecule **3** leads to structural changes. The Al–Al distance in the ring is elongated by 10–12 pm. The terminal Al–P_t distance increases by about 3 pm, while the bridging Al–P_b distances increase by 6–7 pm. The long Al–Al distance is a very soft bonding parameter due to the flexible ring structure in the comparison of two possible structures with the experimental X-ray structure; we shall focus on the Al–P bonds. For one of the possible compounds, **2**, calculations by all functionals give Al–P bond lengths that are 0–3 pm shorter than those in the crystal structure of the yet unknown four-membered-ring compound. For hypothetical compound **3**, however, all calculated Al–P bond lengths are 3–5 pm longer than those in the crystal structure. All three functionals used in the present work overestimated the Al–P bond lengths of butterfly structure **1** by 3–4 pm in comparison with experimental values. Both possible species, **2** and **3**, agree with the experimental X-ray structure to within ±3 pm, and we cannot rule out either of the two.

One would expect that DFT calculations of both **2** and **3** would overestimate the Al–P bond lengths in comparison with experiment, because this happened for butterfly structure **1**. If this were indeed the case, hypothetical compound **3**, in which the SOMOs are saturated with H atoms, would be a good candidate for the compound that was synthesised. However, the computed UV/Vis spectrum of **3** does not lend support to the colour of the synthesised species (vide infra), and there may be other reasons for the seemingly too short Al–P bond lengths in the DFT calculations of **2**. For example, interactions between molecules of **2** in the crystal could have led to elongations of the Al–P bonds, such that the X-ray data for the crystal show longer distances than those for an isolated diradical **2**. In our calculations, the related diradicals Al_2R_4 with R = PH_2 or PMe_2 even form closed-shell dimers, and the Al–P bonds are elongated in these dimers (see section B) – also saturation with H atoms leads to Al–P bond elongations. A similar case of not yet understood strong interactions of radical species in the crystalline state has recently been described for the Al_7R_6 [R = $N(SiMe_2Ph)_2$] cluster. In this case, the stabilisation in the crystal is so high that it could not be dissolved in common solvents. In contrast, the nonmagnetic $Al_7R_6^-$ anion, 454 kJ mol^{-1} lower in energy than the radical, forms an ionic lattice and can, for example, be dissolved in thf.[11,12]

II.A.3. Further Hypothetical Conformers and Building Units

Besides the butterfly structure of $Al_2(PtBu_2)_4$, we have calculated hypothetical linear conformer **4** (C_2 symmetry, ^1A state), which is similar to the above-mentioned molecule, Al_2R_4 [R = $CH(SiMe_3)_2$],[5] with four terminal $PtBu_2$ groups and an Al–Al σ bond length of 265.1–265.7 pm depending on the DFT functional (see Figure 2 and Table 3). This Al–Al bond is about 4–7 pm longer than that in butterfly structure **1**, showing that the bridging phosphorus in the butterfly causes a more rigid bonding situation. The aluminium atoms are moved closer to their "natural" bond length of about 259.9 pm, which they show, for example,

in the sterically unhindered linear $Al_2(PH_2)_4$ molecule. The bridging in the butterfly form of $Al_2(PH_2)_4$ only shortens the Al–Al distance by 2–3 pm.

Table 3. Calculated structural parameters for linear $Al_2(PtBu_2)_4$ (**4**) and radical fragment **5**. Selected bond lengths [pm] and bond angles [°] are given; for atom numbers, see Figure 2. Geometries are optimised by using the functionals BP86, TPSS and B3LYP with a def2-TZVP basis for Al, P and a def2-SV(P) basis for C, H.

	4			**5**		
	BP86	TPSS	B3LYP	BP86	TPSS	B3LYP
Al1–Al2	265.8	265.1	265.7	–	–	–
Al1–P1	236.4	235.6	236.5	238.9	238.1	239.1
Al1–P2	242.3	241.5	241.9	238.9	238.1	239.1
P1–Al1–P2	115.4	115.7	116.0	115.0	115.0	115.0

Considering relative electronic energies, linear conformer **4** lies 21.6 kJ mol^{-1} (B3LYP/def2-TZVP) above the global minimum. All conformers of $Al_2(PtBu_2)_4$ described so far can be regarded as formally built from radical fragment AlP_2tBu_4 (**5**) (C_2 symmetry, ^{2}A state; for structural details see Table 3). In Figure 4, D_e values for the formations from this radical are shown as obtained computationally at the BP86, TPSS and B3LYP levels (with the def2-TZVP† basis for equilibrium geometries and the def2-TZVP basis for energies). At the B3LYP/def2-TZVP level of theory, the stabilisation energy is 158.0 kJ mol^{-1} for butterfly conformer **1** but only 83.5 kJ mol^{-1} for triplet conformer **2**. Thus, **2** lies 74.5 kJ mol^{-1} above the global minimum as compared to 21.6 kJ mol^{-1} for singlet linear conformer **4**. Since we postulate a diethyl ether stabilised radical AlP_2tBu_4 fragment during the formation of **2**, we have calculated this stabilisation, which is indicated in Figure 4. At the B3LYP/def2-TZVP level of theory, this stabilisation is 13.5 kJ mol^{-1}.

II.A.4. Optical Properties

The absorption bands of compounds **1**–**5** in the spectral range down to the near-UV (≈200 nm) were investigated by the calculation of vertical excitation energies in the framework of time-dependent density functional theory (TD-DFT). The theoretical UV/Vis spectra of **1**, **2** and **3** are shown in Figure 5, Figure 6 and Figure 7, respectively. Note that in the computed spectra, absorptions beyond the highest energy band are absent, because the number of calculated excitations was limited. In contrast, the absence of absorption bands in the low-energy region is due to the fact that the molecules do not absorb in this spectral range. The theoretical results can be compared with the experimental UV/Vis spectrum of compound **1** and the reported colours of the crystals, which were weak yellow for the butterfly and green for the four-membered-ring conformer. As expected, the closed-shell butterfly structure, **1**, shows no absorption in the visible range above 420 nm. There is only one absorption at 418 nm close to the UV range that can explain the weak yellow colour of the crystals. The experimental UV/Vis spectrum has an absorption band with a maximum around 300 nm and a broad shoulder going up to about 460 nm. The calculated absorption spectrum, in comparison, is shifted by about 50 nm and has its absorption maximum at 250 nm, but it can explain the measured absorption band with a shoulder well.

Triplet four-membered-ring compound **2** shows various absorption bands within the visible range. Stronger absorptions are at 460 nm, 478 nm and at about 710 nm. In contrast to this, H-saturated four-membered-ring compound **3**, which has a singlet electronic ground state, does not absorb in the visible range. The absorption spectrum of **3** is similar to that of butterfly **1**. In view of the calculated UV/Vis spectrum, we would expect crystals of compound **3** to be

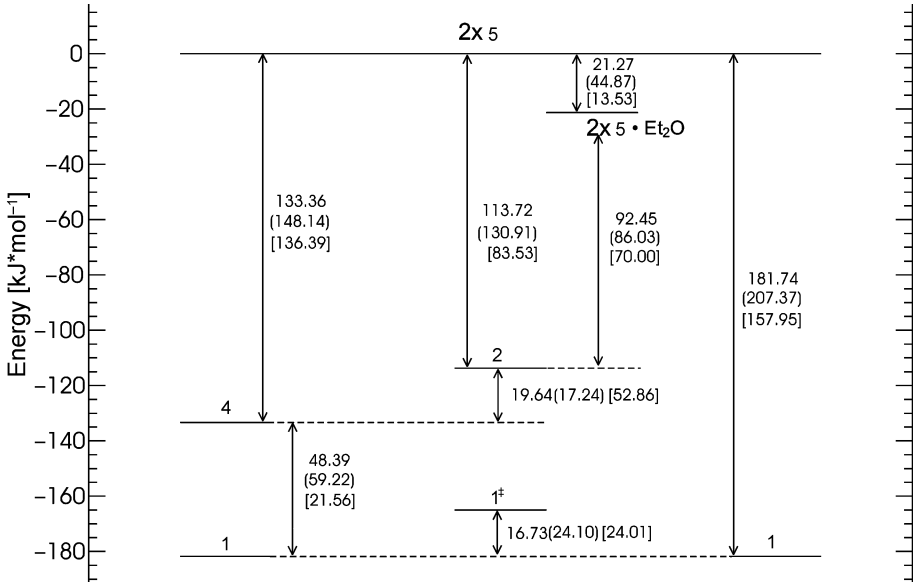

Figure 4. Relative electronic energies of the $Al_2(PtBu_2)_4$ isomers, the AlP_2tBu_4 fragment and TS **1**‡ are given. The diethyl ether stabilised radical of **5** is also shown. Values are BP86/def2-TZVP//BP86/def2-TZVP†, (TPSS/def2-TZVP//TPSS/def2-TZVP†) and [B3LYP/def2-TZVP//B3LYP/def2-TZVP†].

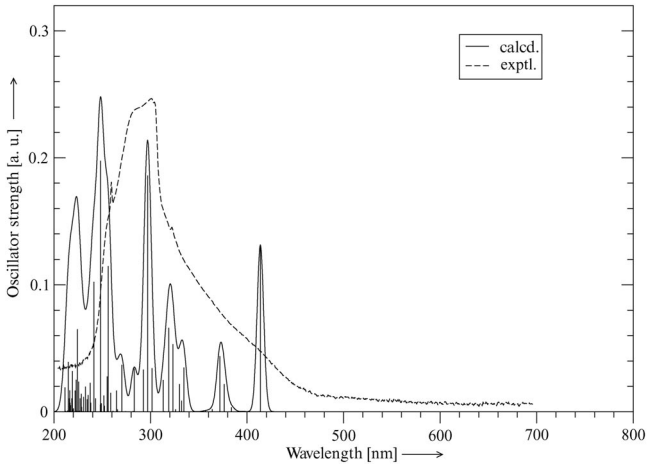

Figure 5. Calculated UV/Vis spectrum of compound **1** at the BP86/def2-TZVP† level of theory. The experimental spectrum is shown as a dashed line.

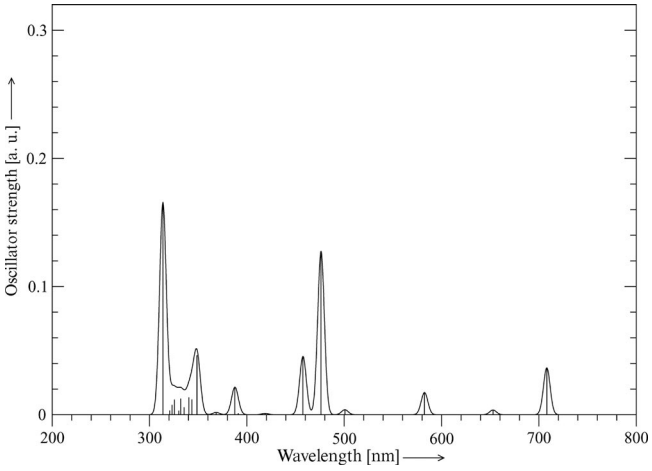

Figure 6. Calculated UV/Vis spectrum of compound **2** at the BP86/def2-TZVP† level of theory.

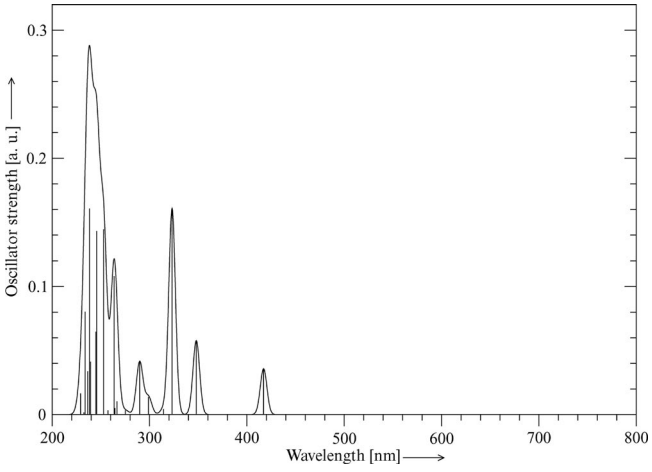

Figure 7. Calculated UV/Vis spectrum of compound **3** at the BP86/def2-TZVP† level of theory.

colourless, not green. Hence, the TD-DFT results support the presence of a triplet state in the experimentally observed four-membered-ring compound as discussed in subsection II.A.2.

II.A.5. CASSCF and MRCI Computations

To investigate the stability of the triplet state of compound **2**, we first performed the following numerical experiment within the single-reference DFT framework. Starting from the B3LYP/def2-TZVP triplet unrestricted Kohn–Sham (UKS) solution (^3A_u state) of **2**, the two SOMOs were localised to give localised molecular orbitals (LMOs) and then the spin was flipped in one of the equivalent LMOs. A symmetry-broken UKS solution (M_S = 0) was obtained in this manner in the equilibrium geometry of **2**. This symmetry-broken state was 11.5 kJ mol^{-1} lower in energy than the triplet state, and when optimising its geometry starting from the triplet geometry, it converged to the (singlet) global minimum of the butterfly structure.

Furthermore, we performed complete-active-space self-consistent-field calculations with two electrons in two orbitals [CASSCF(2,2)] and subsequent internally contracted multireference configuration-interaction calculations (MRCI) for the singlet and triplet states of a model compound, $Al_2(PMe_2)_4$ (in the equilibrium geometry of compound **2**). The results are summarised in Table 4; for more technical details, see section IV. In the MRCI calculations, it turned out that it is sufficient to account for virtual excitations from the CASSCF(2,2) reference space. The singlet–triplet gap does not change much when 58 electrons are correlated in the MRCI (core = 50) treatment. Both CASSCF and MRCI calculations show that the singlet state of the model compound is energetically more stable than the triplet state by 4–6 kJ mol^{-1}.

Table 4. CASSCF(2,2) and internally contracted MRCI energies for model compound $Al_2(PMe_2)_4$.

State	Geometry	Wavefunction	Energy (E_h)	Singlet–triplet gap [kJ mol^{-1}]
Singlet (^1A_g)	**2** (C_i)	CASSCF(2,2)	–2163.899557	
Triplet (^3A_u)	**2** (C_i)	CASSCF(2,2)	–2163.898016	4.0
Singlet (^1A_g)	**2** (C_i)	MRCI (core = 78)	–2163.901432	
Triplet (^3A_u)	**2** (C_i)	MRCI (core = 78)	–2163.899039	6.3
Singlet (^1A_g)	**2** (C_i)	MRCI (core = 50)	–2164.889500	
Triplet (^3A_u)	**2** (C_i)	MRCI (core = 50)	–2164.887098	6.3

The results of this subsection let us expect that monomer **2**, as a triplet diradical, has a short lifetime in solution. There may be two possible mechanisms for stabilisation. Firstly, a spin-flip may occur near the crossing point of the singlet and triplet potential energy surfaces (PESs) – for which the barrier is unknown – after which the molecule would end up in the butterfly form, **1**. Secondly, the triplet diradical could form dimers or oligomers and in this manner be stabilised in the crystal. Although the sterically de-

manding P*t*Bu$_2$ ligands seem to prevent full dimerisation of **2**, as observed for [Al$_2$(O*t*Bu)$_4$]$_2$ in the next subsection, a certain stabilisation may have occurred in the crystal. At this point, we can rule out neither **2** nor **3** as candidates that may explain the X-ray structure of the four-membered ring.

II.B. [Al$_2$(O*t*Bu)$_4$]$_2$

A multicentre aluminium complex with four metal centres has been synthesised by us in still ongoing experiments[8] with the sterically less demanding substituent O*t*Bu instead of P*t*Bu$_2$. We optimised the structure of [Al$_2$(O*t*Bu)$_4$]$_2$ (**6**) at the BP86/def2-TZVP† and B3LYP/def2-TZVP† levels of theory. The structure is displayed in Figure 8, and selected bond lengths and angles are given in Table 5. Compound **6** displays D_2 symmetry, a ^{1}A ground state and a structure in which the four metal centres lie almost in a plane (with a dihedral angle of 2.3°). Two pairs of Al atoms are bridged by two O*t*Bu groups each, which leads to two connected butterfly units. The Al1–Al2 distance within a butterfly unit is 275.5 pm (B3LYP/def2-TZVP†), which is significantly longer than the Al1–Al3 distance of 261.3 pm that connects the two butterfly units. Thus, the bonding situation can best be described by the formation of new bonds between the Al atoms of different monomers, thereby weakening the intramolecular Al–Al bonds. This is underlined by an analysis of the frontier orbitals (HOMO and HOMO–1), which have their main contributions between the Al1 and Al3 atoms (and between Al2 and Al4) but no significant electron density between the Al1 and Al2 atoms (or between Al3 and Al4; Figure 8).

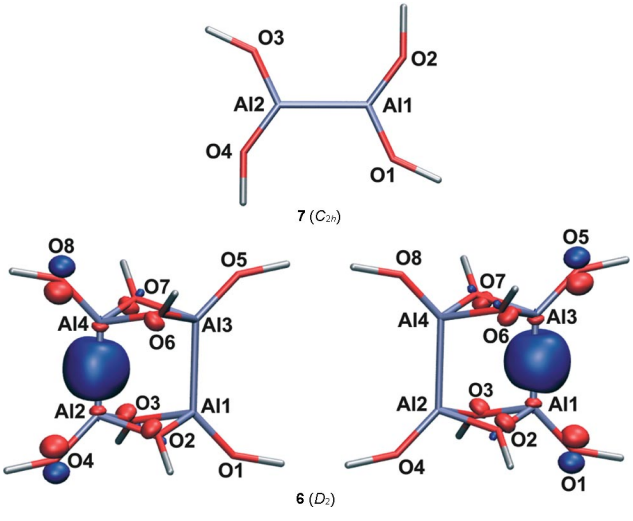

Figure 8. Structures of dimer [Al$_2$(O*t*Bu)$_4$]$_2$ (**6**) and monomer **7**. Localised frontier orbitals (equivalent HOMO and HOMO–1) are plotted (B3LYP/def2-TZVP†). For clarity, only the tertiary carbon atoms of the *t*Bu groups are shown (in silver).

Table 5. Comparison of calculated (BP86/def2-TZVP† and B3LYP/def2-TZVP†) and experimental structural parameters for dimer [Al$_2$(O*t*Bu)$_4$]$_2$ (**6**). Calculated structural parameters for monomer **7** are also shown. Selected bond lengths [pm] and bond angles [°] are given. For numbering of atoms, see Figure 8.

	BP86	B3LYP	Exptl.
	6		**6**
Al1–Al2	277.5	275.5	273.8
Al1–Al3	262.1	261.3	261.7
Al1–O1	173.2	171.6	170.4–170.8
Al1–O2	190.6	189.7	186.4–188.5
Al2–O2	190.1	189.2	186.5–188.0
Al1–O2–Al2	93.6	93.3	93.3–94.5
O2–Al1–O3	80.8	80.8	80.4–80.5
	7		
Al1–Al2	255.7	254.9	–
Al1–O1	171.1	169.5	–
Al1–Al2–O3	114.3	115.3	–
Al1–Al2–O4	127.8	126.5	–
O1–Al1–O2	118.0	118.2	–

These findings agree with the fact that linear conformer **7** (C_{2h} symmetry, ^1A_g state) is a minimum on the PES of Al$_2$(O*t*Bu)$_4$, whereas the butterfly form itself is not a stable structure. In the global minimum of **7**, all of the four oxygen atoms lie in the same plane (eclipsed orientation). The dimerisation of Al$_2$(O*t*Bu)$_4$ causes a substantial elongation of the Al–Al bonds by about 6.4 pm and still by 2.1 pm (Al–O) for the terminally bound O*t*Bu groups for steric reasons. This latter result explains why stable dimers (Al$_2$R$_4$)$_2$ are found only for R = PH$_2$ and R = Me$_2$, while the two aluminium centres cannot come close enough with R = P*t*Bu$_2$ to form a stable dimerisation product.

Nonetheless, the electronic interaction between two Al$_2$R$_4$ moieties containing small ligands (R = PH$_2$, PMe$_2$) may also be present in the crystalline state of **2** (R = P*t*Bu$_2$) in some form but to a much smaller extent. Since the interaction (oligomerisation) between species such as **2** will result in bond elongations (in comparison with the monomeric form) due to the increased coordination number, the shorter Al–P bond lengths calculated by DFT for monomer **2** in the gas phase (in comparison with the X-ray structure of the crystal) may be a consequence of such an interaction in the crystal.

II.C. Al$_2$F$_4$, Al$_2$Cl$_4$ and Dimerisation Products – Model Compounds for Different Bonding Motifs in Al$_2$R$_4$ Species Containing Bridging Ligands

II.C.1. Al$_2$F$_4$ Conformers and Dimer (Al$_2$F$_4$)$_2$

Although Al$_2$Br$_4$ and Al$_2$I$_4$ have been known as donor-stabilised species[6,7] for more than a decade, donor-free Al$_2$X$_4$ molecules have never been discussed, which is not surprising when experimental difficulties are considered.[7] Only AlCl$_2$ has been described under matrix and special synthesis conditions,[13] but these results have been discussed critically.[6] Nevertheless, in an attempt to understand the bonding in the above-mentioned Al$_2$R$_4$ species

and their oligomerisation products, we have chosen aluminium halogenides Al_2X_4 as model compounds to investigate different isomers with ligand-bridged and directly σ-bonded aluminium centres. The halogens X = F and X = Cl were chosen to be able to tune the range of possible Al–Al distances and thus increase the variety of possible structures. The dimerisation to $(Al_2X_4)_2$ was also investigated. For the structures and bonding details of the monomeric isomers and dimers of Al_2X_4, refer to Figure 9 and Figure 10 as well as to Table 6 and Table 7. Standard reaction enthalpies, ΔH_r^0 (298 K), for the dimerisation reactions of the different Al_2X_4 (X = F, Cl) conformers to form $(Al_2X_4)_2$ are shown in Table 8. Moreover, to put these computed enthalpies of reaction into perspective, we have calculated the analogous enthalpies for the reactions

$2\ AlF_3 + 2\ AlF \rightarrow (Al_2F_4)_2$

and

$2\ AlCl_3 + 2\ AlCl \rightarrow (Al_2Cl_4)_2$,

for which the standard enthalpies of formation of the reactants are known experimentally.[14] For the formation of $(Al_2F_4)_2$, the reaction enthalpies are –388.2, –369.6 and –495.4 kJ mol^{-1} at the BP86/def2-TZVPP, B3LYP/def2-TZVPP and MP2/aug-cc-pwCVTZ//B3LYP/def2-TZVPP levels, respectively. For $(Al_2Cl_4)_2$, the corresponding values are –307.2, –256.8 and –383.9, respectively.

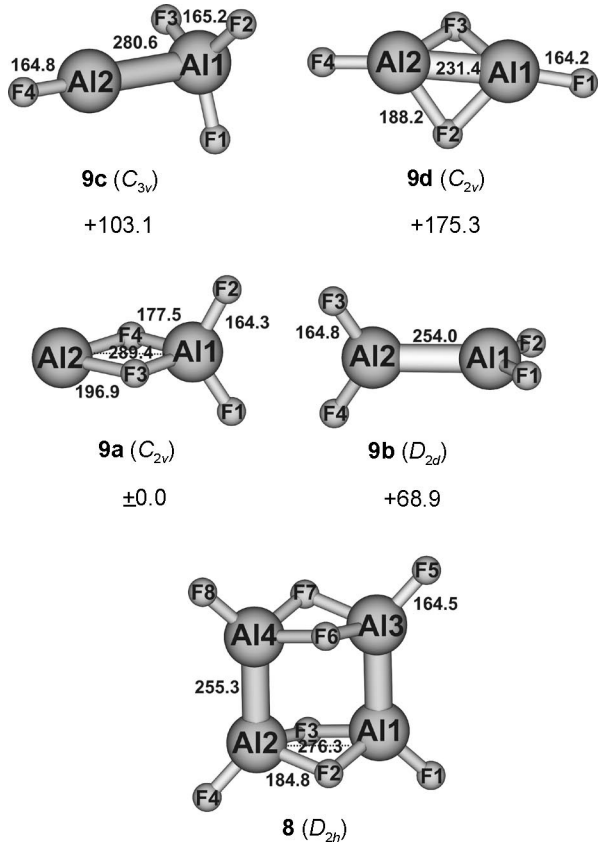

Figure 9. Geometries of dimer $(Al_2F_4)_2$ (**8**) and the isomeric monomers of Al_2F_4, **9a**–**d**. The given bond lengths [pm] and relative energies [kJ mol^{-1}] are calculated at the B3LYP/def2-TZVPP level of theory.

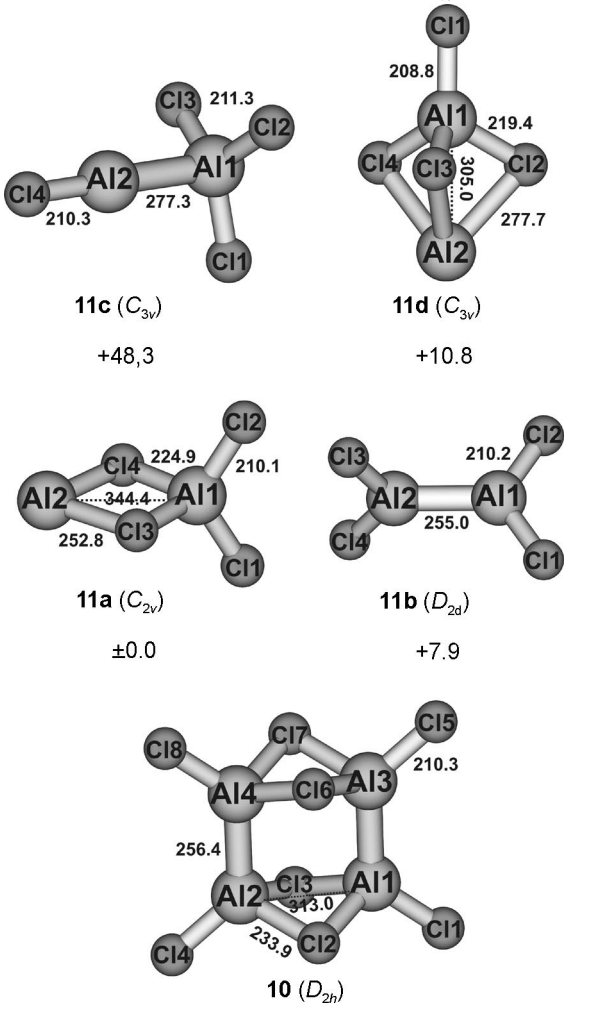

Figure 10. Geometries of dimer $(Al_2Cl_4)_2$ (**10**) and the isomeric monomers of Al_2Cl_4, **11a**–**d**. The given bond lengths [pm] and relative energies [kJ mol^{-1}] are calculated at the B3LYP/def2-TZVPP level of theory.

Table 6. Calculated (BP86/def2-TZVPP and B3LYP/def2-TZVPP) structural parameters for compounds $(Al_2F_4)_2$ (**8**) and $(Al_2Cl_4)_2$ (**10**). Selected bond lengths [pm] and bond angles [°] are given. X denotes F or Cl. For numbering of atoms, see Figures 9 and 10.

	8		**10**	
	BP86	B3LYP	BP86	B3LYP
Al1–Al2	276.2	276.3	309.5	313.0
Al1–Al3	255.5	255.3	256.9	256.4
Al1–X1	165.7	164.5	210.9	210.3
Al1–X2	186.2	184.8	234.0	233.9
Al1–X2–Al2	95.7	96.7	82.8	84.0
X2–Al1–X3	79.5	78.9	88.0	87.3
X1–Al1–Al2	136.3	137.3	129.1	129.8

Analogous to compound $[Al_2(OtBu)_4]_2$ (**6**), the same structure was found for $(Al_2F_4)_2$ (**8**) (D_{2h} symmetry, ^1A_g state), where the nonbonding Al–Al distances within the butterfly elements are 276.3 pm (B3LYP/def2-TZVPP), and the Al–Al σ bond lengths are 255.3 pm. In contrast to **6**, all metal centres lie within a plane in **8**, which causes an additional σ_h plane. The most stable monomer is conformer

Table 7. Comparison of calculated (BP86/def2-TZVPP and B3LYP/def2-TZVPP) structural parameters for the monomeric isomers of Al_2F_4 (**9a**–**d**) and Al_2Cl_4 (**11a**–**d**). Selected bond lengths [pm] and bond angles [°] are given. X denotes F or Cl. For numbering of atoms, see Figures 9 and 10.

	Al_2F_4		Al_2Cl_4	
	BP86	B3LYP	BP86	B3LYP
	9a		**11a**	
Al1–Al2	289.9	289.4	341.9	344.4
Al1–X1	165.4	164.3	210.9	210.1
Al1–X3	179.1	177.5	225.5	224.9
Al2–X3	197.7	196.9	251.0	252.8
Al1–X3–Al2	100.5	101.1	91.5	92.1
X1–Al1–X2	121.1	120.9	119.5	119.1
X3–Al1–X4	84.2	83.8	94.4	94.5
X3–Al2–X4	74.8	74.0	82.5	81.5
	9b		**11b**	
Al1–Al2	254.7	254.0	255.5	255.0
Al1–X1	166.0	164.8	210.8	210.2
X1–Al1–Al2	120.6	120.8	121.0	121.1
X1–Al1–X2	118.9	118.3	118.1	117.9
	9c		**11c**	
Al1–Al2	277.0	280.6	273.2	277.3
Al1–X1	166.5	165.2	212.0	211.3
Al2–X4	166.0	164.8	211.1	210.3
X1–Al1–X2	118.4	118.3	117.6	117.5
X1–Al1–Al2	97.5	97.8	99.5	99.2
	9d			
Al1–Al2	233.1	231.4	–	
Al1–X1	165.5	164.2	–	
Al1–X2	189.9	188.2	–	
Al1–X2–Al2	75.7	75.9	–	
X1–Al1–Al2	166.9	166.7	–	
			11d	
Al1–Al2		–	300.8	305.0
Al1–X1		–	209.2	208.8
Al1–X2		–	220.0	219.4
Al2–X2		–	273.9	277.7
Al1–X2–Al2		–	74.1	74.7
X1–Al1–X2		–	118.8	118.6

Table 8. Calculated reaction enthalpies, ΔH_r^0 (298 K), for the dimerisation reaction of isomeric monomers **9a**–**d** and **11a**–**d** [$2Al_2F_4 \rightarrow (Al_2F_4)_2$ and $2Al_2Cl_4 \rightarrow (Al_2Cl_4)_2$, respectively] at the BP86/def2-TZVPP, B3LYP/def2-TZVPP and MP2/aug-cc-pwCVTZ levels of theory. Enthalpies are in kJ mol^{-1}.

	$2Al_2F_4 \rightarrow (Al_2F_4)_2$				$2Al_2Cl_4 \rightarrow (Al_2Cl_4)_2$			
	9a	**9b**	**9c**	**9d**	**11a**	**11b**	**11c**	**11d**
BP86	–123.1	–239.9	–311.6	–415.4	–141.0	–159.3	–236.4	–148.5
B3LYP	–99.9	–237.7	–306.1	–450.5	–112.6	–128.4	–209.1	–134.1
MP2	–241.0	–386.8	–458.1	–725.8	–174.4	–227.4	–296.5	–183.7

9a (C_{2v} symmetry, $^1A_1$ state), in which two fluorine atoms are terminally bound to the same aluminium atom. The other two fluorine atoms asymmetrically bridge the two metal centres. This leads to a very long nonbonding metal–metal distance of 289.4 pm relative to 276.3 pm (B3LYP/def2-TZVPP) in the more rigid dimer. Formally, conformer **9a** may be interpreted as composed of an $[Al^{III}F_4]^-$ anion and an $[Al^I]^+$ cation. The calculated charges in a natural population analysis (NPA) of +2.16*e* on Al1, +0.87*e* on Al2 and –0.74*e* on F1 and F2, and –0.78*e* on F2 and F3 support this interpretation with a covalent contribution of about 30% (see also Table 9).

Table 9. Atomic charges based on the natural population analysis (NPA) for the different conformers of Al_2F_4 and Al_2Cl_4, obtained at the B3LYP/def2-TZVPP level. Charges are in units of *e*.

	Al_2F_4				Al_2Cl_4			
	9a	**9b**	**9c**	**9d**	**11a**	**11b**	**11c**	**11d**
Al1	+2.160	+1.500	+1.971	+1.490	+1.426	+1.045	+1.153	+1.386
Al2	+0.869	+1.500	+1.080	+1.490	+0.756	+1.045	+1.021	+0.741
X1	–0.738	–0.750	–0.751	–0.744	–0.522	–0.522	–0.521	–0.501
X2	–0.738	–0.750	–0.751	–0.746	–0.522	–0.522	–0.521	–0.542
X3	–0.777	–0.750	–0.751	–0.746	–0.569	–0.522	–0.521	–0.542
X4	–0.777	–0.750	–0.799	–0.744	–0.569	–0.522	–0.611	–0.542

Linear conformer **9b** (D_{2d} symmetry, $^1A_1$ state) is about 73 kJ mol^{-1} higher in energy than **9a** (MP2/aug-cc-pwCVTZ). It has a σ bond of 254 pm between the two aluminium centres, and the four terminally bound fluorine atoms are oriented in a staggered conformation. The charge on both aluminium centres is +1.50*e*. About 36 kJ mol^{-1} (MP2/aug-cc-pwCVTZ) above **9b** lies the conformer **9c** (C_{3v} symmetry, $^1A_1$ state). Formally, this conformer consists of $Al^{III}F_3$ and Al^IF units with a largely ionogenic Al–Al bond. The calculated NPA charges of +1.97*e* on Al1, –0.75*e* on F1, F2 and F3, +1.08*e* on Al2, and –0.80*e* on F4 in conjunction with the long Al–Al bond length of 280.6 pm support this formulation. Butterfly conformer **9d**, (C_{2v} symmetry, $^1A_1$ state) with a dimerisation enthalpy of –450.5 kJ mol^{-1} (B3LYP/def2-TZVPP), is very unstable and only a minimum on the B3LYP potential energy surface. The Al–Al σ bond length of 231.4 pm is extremely short compared to those found in the other structures, which range from 254.0 pm in **9b** to 255.3 pm in **8**. At the BP86 level, this structure is a saddle point (i.e., it displays one imaginary frequency). The restricted Hartree–Fock solution for this conformer reveals a triplet instability and explains the large deviation of the MP2 dimerisation enthalpy from the DFT results.

II.C.2. Al_2Cl_4 Conformers and Dimer $(Al_2Cl_4)_2$

The conformers of Al_2Cl_4 and dimer $(Al_2Cl_4)_2$ with the larger and more polarisable chloride structurally reveal a similar behaviour to that of their counterparts with fluoride, but there are a few differences to be noted. Firstly, all Al_2Cl_4 conformers lie energetically much closer together, all within about 60 kJ mol^{-1}. The butterfly structure that was found for Al_2F_4 at the B3LYP/def2-TZVPP level is not stable with the chloride ligand, since the very short Al–Al distance is not feasible with chloride. On the other hand, besides structure **11a** (C_{2v} symmetry, $^1A_1$ state), there exists another conformer with the $[Al^{III}Cl_4]^-$ $[Al^I]^+$ motif, **11d**, with C_{3v} symmetry ($^1A_1$ state) and only about 5 kJ mol^{-1} higher in energy. This C_{3v} symmetry corresponds to the experimental structures of, for example, $GaGaCl_4$[15,16] and $KAlCl_4$ in the gas phase.[17]

While the calculated atomic charges (Table 9) for conformers **11a** and **11d** are comparable, the bridged Al–Al distance of 305.0 pm in **11d** is almost 40 pm shorter than that in **11a**. The direct Al–Al σ bonds that are found in compounds **10** and **11b** are only slightly affected by the ligand. We find a marginal elongation of about 1 pm in the structures with the chloride ligand, and as expected, the NPA shows an increased covalent contribution for the chloride ligands.

II.D Mg_2Cl_2 and Dimerisation Products

II.D.1. Structures

Starting from $(Al_2Cl_4)_2$ described in the previous section and removing the terminal chloride ligands, one ends up with the stable ionic compound $(Al_2Cl_2)_2^{4+}$ (**14**) (D_{2h} symmetry, ^1A_g state), whose structure is shown in Figure 11. Compound **14** is isoelectronic with the neutral molecule $(Mg_2Cl_2)_2$, where the magnesium centres have the rare oxidation state of Mg^I. Although Mg_2Cl_2 has been characterised theoretically[9] and, very recently, experimentally,[18] nothing is known about oligomeric species. Therefore, we have optimised the structure of $(Mg_2Cl_2)_2$ (**12**) (D_{2h} symmetry, ^1A_g state) in comparison with the two monomeric conformers, **13a** and **13b**, which are shown in Figure 11.

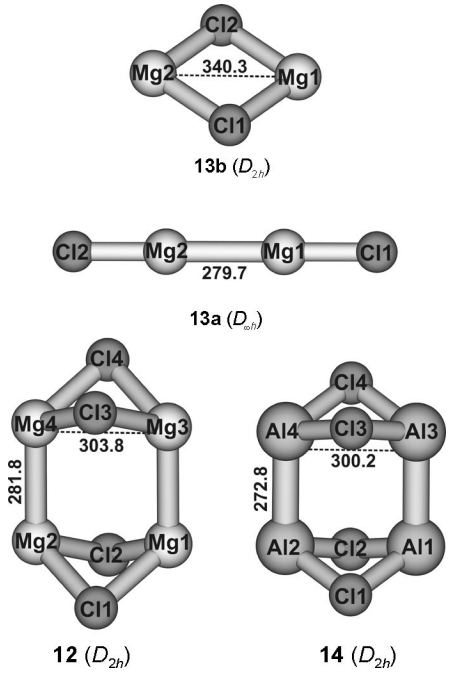

Figure 11. Geometries of $(Mg_2Cl_2)_2$ (**12**) and the isomeric monomers of Mg_2Cl_2, **13a**,**b**. Isoelectronic ion $(Al_2Cl_2)_2^{4+}$ (**14**) is also given. Metal–metal distances [pm] in the different compounds are calculated at the B3LYP/def2-TZVPP level of theory.

Similar to $(Al_2X_4)_2$ and $[Al_2(OtBu)_4]_2$, compound **12** consists of two connected butterfly units with a nonbonding Mg–Mg distance of 303.8 pm within each butterfly. Two Mg–Mg σ bonds of 281.8 pm connect the two butterflies. This Mg–Mg σ bond is 2 pm longer than that in linear monomer **13a** ($D_{\infty h}$ symmetry, $^1\Sigma_g^+$ state). All structural parameters can be found in Table 10. In rhombic conformer **13b** (D_{2h} symmetry, ^1A_g state), the two metal centres are bridged by two chloride ligands, which gives rise to a nonbonding Mg–Mg distance of 340.3 pm. Compound **13b** is only a minimum with respect to nuclear degrees of freedom. The restricted DFT (BP86, B3LYP) as well as the restricted Hartree–Fock solutions show a triplet instability.

Table 10. Structural parameters of $(Mg_2Cl_2)_2$ (**12**) and the monomeric isomers Mg_2Cl_2 (**13a**,**b**) as well as the isoelectronic ion Al_4Cl^{4+} (**14**) are given. In addition, structural parameters of the two isomers **15a**,**b** of the higher condensation product $(Mg_2Cl_2)_4$ are shown. Selected bond lengths [pm] and bond angles [°] at BP86/def2-TZVPP and B3LYP/def2-TZVPP levels of theory. For numbering of atoms, see Figures 11 and 12.

	BP86	B3LYP	BP86	B3LYP
	13a		**13b**	
Mg1–Mg2	281.1	279.7	337.1	340.3
Mg1–Cl1	221.5	220.8	247.8	240.3
Mg1–Cl1–Mg2	0.0	0.0	85.7	90.1
Cl1–Mg1–Cl2	0.0	0.0	94.3	89.9
	12		**14**	
Mg1–Mg2	300.5	303.8	299.1	300.2
Mg1–Mgt3	282.7	281.8	274.7	272.8
Mg1–Cl1	245.6	245.2	229.0	228.2
Mg1–Cl1–Mg2	75.4	76.6	81.6	82.3
Cl1–Mg1–Cl2	87.7	87.3	89.7	89.2
	15a		**15b**	
Mg1–Mg2	342.7	355.3	350.4	359.7
Mg1–Mg3	284.9	283.0	282.3	281.7
Mg1–Mg6	334.2	352.1	495.6	508.7
Mg1–Cl1	242.0	242.0	242.3	242.1
Mg1–Cl1–Mg2	90.1	94.4	92.6	96.0
Mg1–Cl2–Mg6	87.3	93.4	–	

Larger clusters of $(Mg_2Cl_2)_x$ are of interest with respect to the limit of solid MgCl. We have therefore investigated the structures and reaction enthalpies of the cluster with $x = 4$. The structures are shown in Figure 12, and bond parameters are given in Table 10. The global minimum is conformer **15a** (D_{2d} symmetry, $^1A_1$ state) with two Mg_4Cl_2 hexagons rotated by 90° with respect to each other and connected by bridging chloride ligands. Only 11.8 kJ mol^{-1} (MP2/aug-cc-pwCVTZ) higher in energy lies the highly

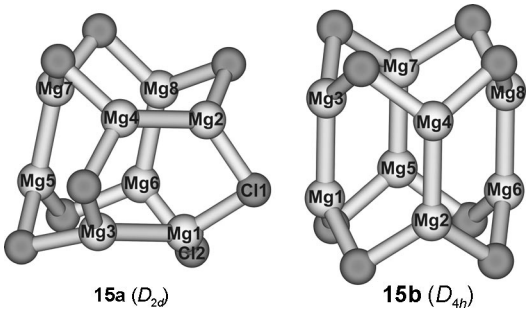

Figure 12. Geometries of the two $(Mg_2Cl_2)_4$ isomers, **15a**,**b**. The highly symmetric isomer, **15b**, is only 11.8 kJ mol^{-1} less stable than **15a** (MP2/aug-cc-pwCVTZ).

symmetric conformer **15b** (D_{4h} symmetry, $^1A_{1g}$ state). Here, the Mg_4Cl_2 hexagons are coplanar. While the Mg–Mg σ bond length of 281.7 pm in the highly symmetric compound $(Mg_2Cl_2)_4$ (**15b**) is the same as that in the smaller compound, $(Mg_2Cl_2)_2$ (**12**), this bond is 1.3 pm longer in global minimum conformer **15a**. Thus, in **15a**, the Mg–Mg σ bond is 3.3 pm longer than that in linear Mg_2Cl_2 monomer **13a**.

II.D.2. Energetics

In Table 11, the calculated reaction enthalpies ΔH_r^0 (298 K) of the reaction xMg(g) + xMgCl$_2$ → $(Mg_2Cl_2)_x$ are given for x = 1, 2 and 4. DFT, MP2 and CCSD(T) enthalpies are all exothermic for compounds **12** and **13a**. Furthermore, the most accurate methods, MP2 and CCSD(T), are in good mutual agreement for these compounds. We thus conclude that the MP2 enthalpies for the larger clusters – where the CCSD(T) calculations were not feasible – will be sufficiently accurate. The discrepancies that arise for **13b** are due to triplet instabilities in the restricted DFT and Hartree–Fock wave functions. DFT and also MP2 predict an endothermic reaction, whereas CCSD(T) yields a small but exothermic enthalpy of –8.2 kJ mol^{-1}. In all cases, the clusters gain stabilisation with increasing cluster size. In the case of $(Mg_2Cl_2)_2$ (**12**), the gain is about 128 kJ mol^{-1} [CCSD(T)/aug-cc-pwCVTZ] to 138 kJ mol^{-1} (MP2/aug-cc-pwCVTZ) with respect to linear Mg_2Cl_2 molecule **13a**. The extra stabilisation (dimerisation enthalpy) is 307 kJ mol^{-1} (MP2/aug-cc-pwCVTZ) for $(Mg_2Cl_2)_4$ with respect to $(Mg_2Cl_2)_2$ (**12**).

Table 11. Calculated reaction enthalpies ΔH_r^0 (298 K) for the reactions xMg(g) + xMgCl$_2$ → $(Mg_2Cl_2)_x$ with x = 1, 2 and 4 at BP86/def2-TZVPP, B3LYP/def2-TZVPP, MP2/aug-cc-pwCVTZ and CCSD(T)/aug-cc-pwCVTZ levels of theory. Enthalpies are in kJ mol^{-1}.

	x = 1		x = 2	x = 4	
	13a	**13b**	**12**	**15a**	**15b**
BP86	–51.5	18.8	–205.6	–666.2	–654.7
B3LYP	–44.5	48.1	–163.7	–582.4	–575.7
MP2	–56.8	7.1	–251.5	–810.0	–798.2
CCSD(T)	–56.6	–8.2	–241.3	–	–

The stabilisation energies starting from Mg(g) and $MgCl_2$(g) are so large that, for a reaction of $MgCl_2$(g) with solid Mg(s) in a nonpolar solvent, an exothermic reaction to $(Mg_2Cl_2)_x$ with $x \geq 4$ should proceed since the vaporisation enthalpy of Mg(s) is only 148 kJ mol^{-1}.[14] Furthermore, since Mg_2Cl_2 could be obtained under matrix conditions recently,[18] there may be a chance to gain further stabilisation via an oligomerisation process that finally may end up with solid MgCl. Theoretical and experimental work on this subject is a challenge for future investigations.

III. Summary and Outlook

The focus of the present work has been on the theoretical investigation of recently synthesised dinuclear and tetranuclear aluminium[8] and magnesium[2,4] compounds with exceptional bonding situations or oxidation states: in all cases, one s electron determines the properties of the metal–metal bonded species. We have optimised the structures of various $Al_2(PtBu_2)_4$ and $[Al_2(OtBu)_4]_2$ isomers in several electronic states. Relative electronic energies have been computed with respect to hypothetical building blocks for the compounds. UV/Vis spectra have been calculated for the isomers of $Al_2(PtBu_2)_4$ to provide further theoretical support for characterising the experimentally found compounds.

The isomeric $Al_2(PtBu_2)_4$ species **1** and **2** reported here are examples of species in the field of cyclobutadienyl compounds containing four-membered-ring entities P_2B_2,[19–21] P_2C_2,[22] Ge_2N_2,[23] Sn_2N_2[24] and Si_4,[25] which have been subject to several reviews.[26,27] Of particular interest has been the exceptional electronic structure of **2** with its diradical character. The diradical character in the calculations of the isolated molecules may still be present in the synthesised crystals or may have triggered mutual or other interactions. A final conclusion on whether a diradical structure of $Al_2(PtBu_2)_4$ has been synthesised is not yet possible. Structural and spectroscopic data for compounds **2** and **3** partly lend support to a structurally modified diradical in the crystal, but an intriguing question – to be addressed in future work – is what these interactions could be and how they stabilise a four-membered-ring structure similar to that of calculated compound **2**.

In order to understand the structural diversity (bonding motifs) of Al_2R_4 species, that is, the chemistry of compounds with one s electron for every metal centre, we first investigated dihalides Al_2F_4 and Al_2Cl_4 as simple model compounds containing bridging ligands.

Furthermore, the Al_2X_4 species seem to represent a suitable bridge to the recently presented Mg_2Cl_2 molecules, exhibiting only one electron for every MgCl unit. For the Mg–Mg σ bond between two Mg^I centres, the dissociation energy has been determined by means of experiments as well as DFT calculations to be about 200 kJ mol^{-1}. For further stabilisation of Mg_2Cl_2 molecules during the oligomerisation process, we have theoretically found stabilisation energies of 128 kJ mol^{-1} to 307 kJ mol^{-1} upon going to $(Mg_2Cl_2)_2$ and $(Mg_2Cl_2)_4$, respectively.

Because of the unexpectedly high stability of larger $(MgCl)_x$ clusters, also with respect to disproportionation into Mg(s) and $MgCl_2$(g), it seems worthwhile to perform experiments as well as additional theoretical work in order to find hints for MgCl(s), which is a so far unknown compound.

IV. Computational Details

All DFT and TD-DFT calculations were carried out with the program package Turbomole.[28,29] The MRCI and CASSCF calculations were done with Molpro.[30] The MP2 calculations for the aluminium compounds were performed with Turbomole, and the MP2 and CCSD(T) calculations for magnesium were carried out with Molpro. The programs ECCE builder,[31] Molden[32] and Vmd[33] were used for the preparation, manipulation and visualisation of coordinate files.

The geometries of $Al_2(PtBu_2)_4$ isomers **1**–**4** and monomer **5** were optimised by using the GGA functional BP86,[34–37] the meta-GGA functional TPSS[38,39] and the hybrid functional B3LYP[37,40,41] by applying a def2-TZVP basis set to Al and P atoms and a def2-SV(P) basis set to H and C atoms.[42,43] This mixed basis set is referred to as def2-TZVP† in the text. Single-point energy calculations at these geometries were performed by using the full def2-TZVP basis set for all atoms. Preoptimisations of all structures described so far were carried out without imposing any symmetry (C_1). The structure refinements were performed in the obtained symmetries: C_2 symmetry for **1**, **4** and **5** and C_i for **1**‡, **2** and **3**. A fine integration grid (grid size 4) and weight derivatives were used when refining the structures. The final convergence criteria were set to 10^{-6} E_h/a_0 for the gradient norm and 10^{-9} E_h for the energy change. These hard convergence criteria were necessary to obtain real minimum structures. For all BP86/def2-TZVP† geometries, harmonic vibrational frequencies were calculated analytically to confirm the minimum structures of **1**–**5** and transition state structure **1**‡ with one and only one imaginary frequency resembling the normal mode of the butterfly movement.[44–46] Analogous calculations were done for the $Al_2(OtBu)_4$ dimer and monomer with the functionals BP86 and B3LYP, which resulted in the minimum structures **6** (D_2) and **7** (C_{2h}).

Vertical excitation energies in the UV/Vis spectral range were calculated for compounds **1**–**5** with TD-DFT by using BP86/def2-TZVP†.[47,48] The vertical transition energies in the spectral range 200–800 nm were plotted against the oscillator strengths (line spectra). In addition, Gaussian lineshapes with a half-width at a half-maximum value of 4 nm were plotted to obtain realistic-looking UV/Vis spectra.

Complete-active-space self-consistent-field calculations with two electrons in two orbitals [CASSCF(2,2)] and subsequent internally contracted multireference configuration-interaction calculations (MRCI) were performed for the singlet and triplet states of model compound $Al_2(PMe_2)_4$ in the correlation-consistent polarised valence triple-zeta basis set (cc-pVTZ).[49–55] The structure of the model compound was kept fixed to the equilibrium geometry of **2**. It was obtained from the structure of **2** by replacing the *t*Bu groups by Me groups, thereby placing the hydrogen atoms onto the former C–CH_3 bonds at a (fixed) C–H distance of 110 pm. The CASSCF(2,2) wavefunction for the ^1A_g state of the model for **2** (C_i symmetry) was built from two determinants ($a_g a_g$ and $a_u a_u$), while the corresponding wavefunction for the ^3A_u state was described by just one single determinant ($a_g a_u$). The MRCI calculations were performed in two distinct manners. In one set of calculations, single and double excitations were allowed only from the CASSCF(2,2) reference space. This corresponds to correlating two electrons and freezing 78 doubly occupied orbitals (core = 78; the total number of electrons in the model compound is 158). In the other set of calculations, we also allowed single and double excitations from 28 further valence orbitals, thus correlating 58 electrons and freezing 50 doubly occupied orbitals (core = 50).

The smaller aluminium compounds $(Al_2F_4)_x$ (**8**, **9a**–**9d**) and $(Al_2Cl_4)_x$ (**10**, **11a**–**11d**) with x = 1, 2 and all magnesium compounds $(Mg_2Cl_2)_x$ with x = 1, 2 and 4 were optimised with the functionals BP86 and B3LYP by using a def2-TZVPP basis set for all atoms.[42,56] Again, a fine integration grid (grid size 4) and weight derivatives were used. Here the convergence criteria were chosen as 10^{-5} E_h/a_0 for the gradient norm and 10^{-8} E_h for the energy change. Harmonic vibrational frequencies were calculated analytically, and all of these structures were checked for singlet and triplet instabilities in the wave function.[57] Enthalpies ΔH_r^0 (298 K) were evaluated by thermal correction of binding energies at 0 K (D_0) by using the module Freeh of Turbomole (ideal gas approximation). D_0 values were obtained by zero-point vibrational energy corrections (ZPVE) to the D_e values.

MP2 energies for the smaller aluminium compounds were calculated for the B3LYP/def2-TZVPP optimal geometries by using the module Ricc2 and the "resolution of the identity" (RI) approximation in an aug-cc-pwCVTZ basis set.[53–55,58–62] The auxiliary basis set to approximate the Coulomb integrals and Hartree–Fock exchange in the RI-HF reference wavefunction calculation was def2-QZVPP.[63–65] The MP2 and CCSD(T) energies for the B3LYP/def2-TZVPP optimal geometries of the magnesium compounds were calculated by using an aug-cc-pwCVTZ basis set.[55,62,66–69] A frozen core was chosen as Al(1s), Mg(1s), F(1s) and Cl(1s2s2p). Thermal and ZPVE corrections to MP2 and CCSD(T) energies were based on the B3LYP/def2-TZVPP vibrational frequencies.

All DFT calculations in this work were carried out with the "resolution of the identity" (RI) approximation by applying appropriate auxiliary basis sets.[56,64,70–73]

Acknowledgments

This research has been supported by the Deutsche Forschungsgemeinschaft (DFG) through the Center for Functional Nanostructures (CFN, project nos. C1.3 and C3.3) and by a grant from the Ministry of Science, Research and the Arts of Baden-Württemberg (Az: 7713.14-300). Further support by the Fonds der Chemischen Industrie is gratefully acknowledged.

[1] I. Resa, E. Carmona, E. Gutierrez-Puebla, A. Monge, *Science* **2004**, *305*, 1136.
[2] S. P. Green, C. Jones, A. Stasch, *Science* **2007**, *318*, 1754–1757.
[3] A. Schnepf, H.-J. Himmel, *Angew. Chem.* **2005**, *117*, 3066–3068; *Angew. Chem. Int. Ed.* **2005**, *44*, 3006–3008.
[4] M. Westerhausen, *Angew. Chem.* **2008**, *120*, 2215–2217; *Angew. Chem. Int. Ed.* **2008**, *47*, 2185–2187.
[5] W. Z. Uhl, *Naturforsch. B* **1988**, *43*, 1113.
[6] M. Mocker, C. Robl, H. Schnöckel, *Angew. Chem.* **1994**, *106*, 946–948; *Angew. Chem. Int. Ed. Engl.* **1994**, *33*, 862–863.
[7] C. Dohmeier, D. Loos, H. Schnöckel, *Angew. Chem.* **1996**, *108*, 141–161; *Angew. Chem. Int. Ed. Engl.* **1996**, *35*, 129–149.
[8] P. Henke, T. Pankewitz, W. Klopper, H. Schnöckel, *Angew. Chem.*, in preparation.
[9] Y. Xie, H. F. Schaefer III, E. D. Jemmis, *Chem. Phys. Lett.* **2005**, *402*, 414–421.
[10] A. Velazquez, I. Fernández, G. Frenking, G. Merino, *Organometallics* **2007**, *26*, 4731–4736.
[11] P. Yang, R. Köppe, T. Duan, J. Hartig, G. Hadiprono, B. Pilawa, I. Keilhauer, H. Schnöckel, *Angew. Chem.* **2007**, *119*, 3650–3654; *Angew. Chem. Int. Ed.* **2007**, *46*, 3579–3583.
[12] S. D. Köhler, B. Pilawa, D. Saez de Jauregui, G. Fischer, R. Grubba, A. Schnepf, H. Schnöckel, E. Dormann, *EPL* **2008**, *82*, 37002.
[13] G. A. Olah, O. Farooq, S. M. F. Farnia, M. R. Bruce, F. L. Clouet, P. R. Morton, G. K. S. Prakash, R. C. Stevens, R. Bau, *J. Am. Chem. Soc.* **1988**, *110*, 3231–3238.
[14] M. Binnewies, E. Milke, *Thermochemical Data of Elements and Compounds*, Wiley-VCH, Weinheim, **2002**.
[15] H. Schmidbaur, *Angew. Chem.* **1985**, *97*, 893–904; *Angew. Chem. Int. Ed. Engl.* **1985**, *24*, 893–904.
[16] A. J. Downs, *Chemistry of Aluminium, Gallium, Indium, and Thallium*, Chapman & Hall, London, **1993**.
[17] Y. S. Kalaichev, K. P. Petrov, V. V. Ugarov, *Russ. J. Struct. Chem. (Engl. Transl.)* **1983**, *24*, 811.

[18] R. Köppe, P. Henke, H. Schnöckel, *Angew. Chem.*, accepted.
[19] H. A. D. Scheschkewitz, H. Gornitzka, W. W. Schoeller, D. Bourissou, G. Bertrand, *Science* **2002**, *295*, 1880–1881.
[20] H. A. D. Scheschkewitz, H. Gornitzka, W. W. Schoeller, D. Bourissou, G. Bertrand, *Angew. Chem.* **2004**, *116*, 595–597; *Angew. Chem. Int. Ed.* **2004**, *43*, 585–587.
[21] V. Gandon, J.-B. Bourg, F. S. Tham, W. W. Schoeller, G. Bertrand, *Angew. Chem.* **2008**, *120*, 161–165; *Angew. Chem. Int. Ed.* **2008**, *47*, 155–159.
[22] A. F. E. Niecke, F. Baumeister, M. Nieger, W. W. Schoeller, *Angew. Chem.* **1995**, *107*, 640–642; *Angew. Chem. Int. Ed. Engl.* **1995**, *34*, 555–557.
[23] M. B. C. Cui, M. M. Olmstead, P. P. Power, *J. Am. Chem. Soc.* **2004**, *126*, 6510–6511.
[24] H. Cox, P. B. Hitchcock, M. F. Lappert, L. J.-M. Pierssens, *Angew. Chem.* **2004**, *116*, 4600–4604; *Angew. Chem. Int. Ed.* **2004**, *43*, 4500–4504.
[25] A. Sekiguchi, T. Matsuno, M. Ichinohe, *J. Am. Chem. Soc.* **2001**, *123*, 12436–12437.
[26] H. Grützmacher, F. Breher, *Angew. Chem.* **2002**, *114*, 4178–4184; *Angew. Chem. Int. Ed.* **2002**, *41*, 4006–4011.
[27] F. Breher, *Coord. Chem. Rev.* **2007**, *251*, 1007–1043.
[28] R. Ahlrichs, M. Bär, M. Häser, H. Horn, C. Kölmel, *Chem. Phys. Lett.* **1989**, *162*, 165–169.
[29] *Turbomole* v5.9–v5.10, University of Karlsruhe (TH), **2006**–**2008**.
[30] H.-J. Werner, P. J. Knowles, R. Lindh, F. R. Manby, M. Schütz, P. Celani, T. Korona, G. Rauhut, R. D. Amos, A. Bernhardsson, A. Berning, D. L. Cooper, M. J. O. Deegan, A. J. Dobbyn, F. Eckert, C. Hampel, G. Hetzer, A. W. Lloyd, S. J. McNicholas, W. Meyer, M. E. Mura, A. Nicklass, P. Palmieri, R. Pitzer, U. Schumann, H. Stoll, A. J. Stone, R. Tarroni, T. Thorsteinsson, *Molpro, version 2006.1, A Package of Ab Initio Programs*, **2006**.
[31] G. Black, J. Daily, B. Didier, T. Elsethagen, D. Feller, D. Gracio, M. Hackler, S. Havre, D. Jones, E. Jurrus, T. Keller, C. Lansing, S. Matsumoto, B. Palmer, M. Peterson, K. Schuchardt, E. Stephan, L. Sun, K. Swanson, H. Taylor, G. Thomas, E. Vorpagel, T. Windus, C. Winters, *ECCE, A Problem Solving Environment for Computational Chemistry*, software version 4.0.1, **2006**.
[32] G. Schaftenaar, J. H. Noordik, *J. Comput. Aided Mol. Des.* **2000**, *14*, 123–134.
[33] W. Humphrey, A. Dalke, K. Schulten, *J. Mol. Graphics* **1996**, *14*, 33–38.
[34] S. H. Vosko, L. Wilk, M. Nusair, *Can. J. Phys.* **1980**, *58*, 1200–1211.
[35] J. P. Perdew, *Phys. Rev. B* **1986**, *33*, 8822–8824.
[36] J. P. Perdew, *Phys. Rev. B* **1986**, *34*, 7406.
[37] A. D. Becke, *Phys. Rev. A* **1988**, *38*, 3098–3100.
[38] J. P. Perdew, Y. Wang, *Phys. Rev. B* **1992**, *45*, 13244–13249.
[39] J. Tao, J. P. Perdew, V. N. Staroverov, G. E. Scuseria, *Phys. Rev. Lett.* **2003**, *91*, 146401.
[40] C. Lee, W. Yang, R. G. Parr, *Phys. Rev. B* **1988**, *37*, 785–789.
[41] A. D. Becke, *J. Chem. Phys.* **1993**, *98*, 5648–5652.
[42] F. Weigend, R. Ahlrichs, *Phys. Chem. Chem. Phys.* **2005**, *7*, 3297–3305.
[43] A. Schäfer, H. Horn, R. Ahlrichs, *J. Chem. Phys.* **1992**, *97*, 2571–2577.
[44] P. Deglmann, F. Furche, R. Ahlrichs, *Chem. Phys. Lett.* **2002**, *362*, 511–518.
[45] P. Deglmann, F. Furche, *J. Chem. Phys.* **2002**, *117*, 9535–9538.
[46] P. Deglmann, K. May, F. Furche, R. Ahlrichs, *Chem. Phys. Lett.* **2004**, *384*, 103–107.
[47] R. Bauernschmitt, R. Ahlrichs, *Chem. Phys. Lett.* **1996**, *256*, 454–464.
[48] R. Bauernschmitt, M. Häser, O. Treutler, R. Ahlrichs, *Chem. Phys. Lett.* **1997**, *264*, 573–578.
[49] H.-J. Werner, P. J. Knowles, *J. Chem. Phys.* **1985**, *82*, 5053–5063.
[50] P. J. Knowles, H.-J. Werner, *Chem. Phys. Lett.* **1985**, *115*, 259–267.
[51] H.-J. Werner, P. J. Knowles, *J. Chem. Phys.* **1988**, *89*, 5803–5814.
[52] P. J. Knowles, H.-J. Werner, *Chem. Phys. Lett.* **1988**, *145*, 514–522.
[53] T. H. Dunning Jr, *J. Chem. Phys.* **1989**, *90*, 1007–1023.
[54] R. A. Kendall, T. H. Dunning Jr, R. J. Harrison, *J. Chem. Phys.* **1992**, *96*, 6796–6806.
[55] T. H. Dunning Jr, D. E. Woon, *J. Chem. Phys.* **1993**, *98*, 1358–1371.
[56] F. Weigend, *Phys. Chem. Chem. Phys.* **2006**, *8*, 1057–1065.
[57] R. Bauernschmitt, R. Ahlrichs, *J. Chem. Phys.* **1996**, *104*, 9047–9052.
[58] F. Weigend, M. Häser, *Theor. Chem. Acc.* **1997**, *97*, 331–340.
[59] F. Weigend, M. Häser, H. Patzelt, R. Ahlrichs, *Chem. Phys. Lett.* **1998**, *294*, 143–152.
[60] C. Hättig, *Phys. Chem. Chem. Phys.* **2005**, *7*, 59–66.
[61] F. Weigend, A. Köhn, C. Hättig, *J. Chem. Phys.* **2002**, *116*, 3175–3183.
[62] K. A. Peterson, T. H. Dunning Jr, *J. Chem. Phys.* **2002**, *117*, 10548–10560.
[63] F. Weigend, *Phys. Chem. Chem. Phys.* **2002**, *4*, 4285–4291.
[64] M. Kattannek, PhD Thesis, University of Karlsruhe (TH), **2006**.
[65] F. Weigend, *J. Comput. Chem.* **2008**, *29*, 167–175.
[66] K. Raghavachari, G. W. Trucks, J. A. Pople, M. HeadGordon, *Chem. Phys. Lett.* **1989**, *157*, 479–483.
[67] C. Hampel, K. A. Peterson, H.-J. Werner, *Chem. Phys. Lett.* **1992**, *190*, 1–12.
[68] M. J. O. Deegan, P. J. Knowles, *Chem. Phys. Lett.* **1994**, *227*, 321–326.
[69] K. L. Schuchardt, B. T. Didier, T. Elsethagen, L. Sun, V. Gurumoorthi, J. Chase, J. Li, T. L. Windus, *J. Chem. Inf. Mod.* **2007**, *47*, 1045–1052.
[70] O. Treutler, R. Ahlrichs, *J. Chem. Phys.* **1995**, *102*, 346–354.
[71] K. Eichkorn, O. Treutler, H. Öhm, M. Häser, R. Ahlrichs, *Chem. Phys. Lett.* **1995**, *242*, 652–660.
[72] K. Eichkorn, F. Weigend, O. Treutler, R. Ahlrichs, *Theor. Chem. Acc.* **1997**, *97*, 119–124.
[73] R. Ahlrichs, *Phys. Chem. Chem. Phys.* **2004**, *6*, 5119–5121.

Received: June 19, 2008
Published Online: September 17, 2008

